# Biofiltration field study for cold Fe(II)- and Mn(II)-rich groundwater: accelerated Mn(II) removal kinetics and cold-adapted Mn(II)-oxidizing microbial populations

Sandeepraja Dangeti, Babak Roshani, Brian Rindall, Joyce M. McBeth and Wonjae Chang

## ABSTRACT

Removal of Mn(II) from Fe(II)- and Mn(II)-rich groundwater in cold regions is challenging, due to slow Mn(II) removal kinetics below 15 °C. This study demonstrated onset, acclimation, and acceleration of Mn(II) removal in a two-stage pilot-scale biofilter (Fe and Mn filters) at varying low on-site temperatures (8–14.8 °C). Mn(II) removal commenced at 8 °C in the Mn filter after Fe(II) removal. A shift in redox-pH conditions favored biological Mn(II) removal and Mn(II)-oxidizing bacteria increased. The Mn filter reached steady-state functioning after 97 days, exhibiting high removal efficiencies (97 ± 0.9%). Yet, first-order rate constants ($k$) for Mn(II) removal were low ($10^{-6}$–$10^{-5}$ $min^{-1}$; $t_{1/2}$ = ~40 d). After consecutive backwashes and filter inoculation with backwashed sludge, $k$ remarkably accelerated to 0.21 $min^{-1}$ ($t_{1/2}$ = 3.31 min at 11 ± 0.6 °C). The cold-adapted microbial consortium (51 genera), including *Pseudomonas*, *Leptothrix*, *Flavobacterium*, and *Zoogloea*, cultured from the field-aged biofilter rapidly produced biogenic Mn oxides at 8 °C, confirmed by electron paramagnetic resonance spectroscopy. Birnessite and pyrolusite detected by synchrotron-based powder X-ray diffraction, and a repetitive birnessite-like surface morphology on ripened filter materials, reflected autocatalytic oxidation. Shifting in $k$ indicated the vertical progress of biofilter ripening, which was not limited by low temperature.

**Key words** | accelerated Mn(II) removal, biofiltration, biological Mn(II) oxidation, birnessite, groundwater, Mn(II)-oxidizing bacteria

**Sandeepraja Dangeti**
**Wonjae Chang** (corresponding author)
Department of Civil, Geological and Environmental Engineering,
University of Saskatchewan,
Saskatoon, Saskatchewan,
Canada
E-mail: *wonjae.chang@usask.ca*

**Babak Roshani**
**Brian Rindall**
Delco Water Division,
Delco Automation Inc.,
Saskatoon, Saskatchewan,
Canada

**Joyce M. McBeth**
Department of Geological Sciences,
University of Saskatchewan,
Saskatoon, Saskatchewan,
Canada

## INTRODUCTION

Dissolved manganese in groundwater exists in its reduced form, Mn(II). Excess soluble Mn(II) is a common element of concern in water supplies. Under redox conditions favorable for Mn(II) oxidation, Mn(II) is converted to solid, dark brown Mn(III/IV) oxides, which results in black discoloration and lowers the esthetic quality of drinking water. The deposition of Mn(III/IV) oxides causes scaling and corrosion in water supply infrastructure (Pacini *et al.* 2005).

Biofiltration technology has been widely considered for the treatment of Mn-rich groundwater. Biofiltration promotes microbially mediated Mn(II) oxidation that converts soluble Mn(II) to insoluble Mn(III/IV)-oxide precipitates, which are easily filtered out by filter media in biofiltration systems. However, microbial activity is temperature-dependent. Low temperatures greatly hinder the activity of mesophilic Mn(II)-oxidizing bacteria (MnOB), resulting in long start-up periods and the need for energy-intensive biofiltration (Tekerlekopoulou *et al.* 2013). This is a concern, particularly in vast northern cold-climate regions (e.g., Canada, Alaska, and northern

doi: 10.2166/wqrj.2017.006

China and Europe) (Štembal *et al.* 2005; Cai *et al.* 2016). Previous studies report that Mn(II) removal promoted by MnOB activity and/or Mn-oxide surface coatings on filter materials significantly decreases below 15 °C (Berbenni *et al.* 2000; Cooley & Knocke 2016). The Mn(II) oxidation activity of *Leptothrix discophora* (MnOB) incubated at 8 °C, for example, was suppressed to 50–80% of its oxidation activity at room temperature (Boogerd & de Vrind 1987).

However, at the same time, MnOB are ubiquitous in natural and engineered environments such as the deep sea, rivers, lake sediments, fjords, and water pipes (Tebo *et al.* 2005). Indigenous MnOB tolerant to low temperatures may be abundant or even prevail in cold habitats (Krishnan *et al.* 2009). Enhancing MnOB adapted to low temperatures may be crucial for the onset of Mn(II) oxidation and the generation of biogenic Mn oxides. Those biogenic Mn oxides may then trigger autocatalytic Mn(II) oxidation during biofiltration (Burger *et al.* 2008; Bruins *et al.* 2015a), which may positively influence the kinetics of Mn(II) removal in cold environments. Yet, cold-adapted MnOB capable of rapidly generating Mn oxides at low temperatures have not been extensively reported in previous field studies. In addition, the onset, acclimation, and acceleration of Mn(II) removal under low temperature regimes have not been extensively described in biofiltration studies conducted at field sites.

In this study, a flow-through pilot-scale biofiltration unit containing virgin filter media (anthracite, sand, and gravel) was installed for the field experiment for the treatment of cold Fe(II)- and Mn(II)-rich groundwater. Fe(II) is often naturally abundant when groundwater is rich in Mn(II). Fe(II) oxidation is very thermodynamically favorable and occurs rapidly in the presence of oxygen. However, the Mn(II) oxidation kinetics are very slow or negligible in the absence of biotic and/or abiotic catalysts (Mouchet 1992). This study focuses on Mn(II) removal through a two-stage biofiltration unit at a water treatment plant in the town of Langham (Saskatchewan, Canada), which has an annual mean temperature of ~2 °C. The temperature of the influent groundwater that continuously flowed into the biofiltration unit ranged from 4 to 8 °C, and the effluent temperature of the Mn filter ranged from 8 to 14.8 °C throughout the study. The objective of this study was to demonstrate how Mn(II) oxidation activity commenced, acclimated and accelerated in the biofiltration unit under the low on-site temperature regime. This study also addresses how Mn(II) removal kinetics is related to filter ripening. A cold-adapted MnOB consortium derived from the sufficiently aged Mn filter was investigated.

## MATERIALS AND METHODS

### Natural groundwater

The groundwater source in this field experiment was the Floral formation of the Dalmeny aquifer in Saskatchewan (SK) (Fortin *et al.* 1991), accessed via a groundwater well at the Langham Water Treatment Plant. Water chemistry data for the influent groundwater used in this study are presented in Table 1.

**Table 1** | Operational parameters for the pilot-scale biofiltration unit and water chemistry data for the influent and effluent groundwater

| | | |
|---|---|---|
| Operational parameters | | |
| Flow velocity | 3.21 m/h | |
| Number of backwashes | 9 | |
| Filter depth (cm) | | |
| Head space | 44 | |
| Anthracite | 50 | |
| Fine and coarse sand | 41 | |
| Gravel | 20 | |
| Groundwater chemistry | | |
| | Influent | Mn filter effluent |
| Temperature (°C)[a] | 4–8 | 8–14.8 |
| pH[a] | 7.1 | 7.2–7.8 |
| ORP (mV)[a] | −45 | 300–500 |
| Total Fe (mg/L)[b,c] | 2.81 ± 0.02 | 0.002 ± 0.001 |
| Total Mn (mg/L)[b,c] | 0.88 ± 0.01[d] | <0.001 |
| $NH_3$ (mg/L)[b,c] | 0.53 | 0.13 |
| $NO_3$ (mg/L)[b,c] | 0.04 | 2.2 |

[a]Measured using the sensors on-site.
[b]Sampled at 110 days.
[c]ICP-OES analyses.
[d]0.88 ± 0.01 mg/L in groundwater influent; and 0.84 mg/L in Fe filter effluent.

### Biofiltration system

Figure S1 in the Supplementary material (available with the online version of this paper) illustrates the schematic diagram for the biofiltration unit. The biofiltration unit was designed to remove Fe(II) in the first filter (Fe filter) and Mn(II) in the second filter (Mn filter). From top to bottom, the two filter columns contained four layers of filter media: granular anthracite, fine sand, coarse sand, and gravel. An aeration tank with an air compressor was installed between the Fe and Mn filters to aerate the groundwater. The biofiltration experiment was conducted over six months from July 2014 to January 2015, to include both a summer and a winter season. The operational parameters for the biofiltration unit are summarized in Table 1. Detailed information about the biofiltration operation is available in the Supplementary material.

### On-site monitoring and chemical analyses

During biofiltration, water chemistry data were collected on-site for the effluents of the two biofilters: Fe(II) and Mn(II) concentrations, temperature, pH, oxidation-reduction potential (ORP), and dissolved oxygen (DO). Colorimetric analyses were used to measure Fe(II) and Mn(II) concentrations (Hach Methods 8146 and 8149, respectively). Two sets of three probes were installed at the outlet of each biofilter (Hach-PD2P1, Hach-RD1P5, and Hach-5540D0C) to monitor pH, ORP, DO, and temperature. The formation of Mn oxides on the filter media in the biofiltration unit was assessed on-site using the Leucoberbelin blue I (LBB) colorimetric assay (Sigma-Aldrich Canada). For water samples collected from the Mn filter, off-site analyses were performed using inductively coupled plasma optical emission spectroscopy (ICP-OES) to precisely confirm the changes in Fe(II) and Mn(II) concentrations in the groundwater before and after the biofiltration treatment. Detailed information about effluent sampling (triplicate) and data analyses, including statistical analyses, is presented in the Supplementary material.

### Viability, metabolic activity, and cold-adapted MnOB consortium culturing

The number of viable MnOB, the most probable number (MPN), and adenosine triphosphate (ATP) concentrations were determined as similarly described in relevant previous studies (Tebo *et al.* 2007; Granger *et al.* 2014). Cold-adapted MnOB consortia were cultured at 8 °C using backwash water collected on day 110 from the Mn filter. Further information for the culture-dependent analyses above is presented in the Supplementary material.

Genomic DNA was extracted from the cultured consortium using PowerWater® DNA Isolation Kits (MoBio Laboratories). Extracted DNA was sent to RTLGenomics (Lubbock, Texas) for high-throughput amplicon sequencing using the *Illumina*-MiSeq platform. Raw sequence reads were processed using the MOTHUR software package, version v.1.32.0, following the standard operating procedure for MiSeq analyses (Schloss *et al.* 2009). 16S rRNA gene amplicons (pair ends) from the enriched MnOB consortium were deposited in the European Nucleotide Archive (ENA) under project number PRJEB15479, and accession numbers ERS1360945 and ERS1360944.

### Mn-oxide characterization

To characterize the surface morphology and elements of the solid precipitates and filter materials, analyses were conducted using scanning electron microscopy with energy dispersive X-ray spectrometry (SEM/EDS; Hitachi S3000-N SEM with a Quartz PCI XOne SSD X-ray analyzer). An electron paramagnetic resonance (EPR) spectroscopy analysis was performed for the precipitates obtained from the culturable MnOB consortium (Supplementary material). Synchrotron-based powder X-ray diffraction (PXRD) analyses were conducted using the Canadian Macromolecular Crystallography Facility's bending magnet beamline (CMCF-BM, 08B1-1) at the Canadian Light Source (CLS). Detailed information about the data processing is available in the Supplementary material.

### Mn(II) removal kinetics

Mn(II) removal kinetics is expressed using the following first-order kinetic model that considers empty bed contact time (EBCT), as similarly described in previous studies (Katsoyiannis & Zouboulis 2004; Yang *et al.* 2015; Zeng

et al. 2015; Cheng et al. 2016).

$$\frac{d[Mn(II)]_t}{dt} = -k[Mn(II)]_t$$

In the equation above, $k$ is the first-order rate constant ($min^{-1}$) for the overall removal of Mn(II), which may include biological and/or physico-chemical removal. $[Mn]_t$ is the concentration of Mn(II) at the EBCT. The EBCT is the amount of time an influent to be treated is in contact with the filter media in a vertical filter column. The EBCT is calculated as follows:

$$Empty\ Bed\ Contact\ Time\ (EBCT) = \frac{Volume\ (L)}{Flow\ rate\ \left(\frac{L}{min}\right)}$$

The Mn(II) concentrations in samples collected from the four sampling ports of the Mn filter were measured for the kinetic analyses. Temporal changes in the vertical distribution of Mn(II) concentrations were assessed using the four sampling ports installed vertically along the biofiltration unit at varying depths. Contour maps for Mn(II) concentrations in the Mn filter were generated using Surfer 13 (Golden Software).

## RESULTS AND DISCUSSION

### Start-up and steady-state functioning of the biofilter

Dissolved Fe(II) concentrations in the groundwater rapidly decreased through the Fe filter (Figure 1(a)). Fe(II) concentrations in the effluent stream of the Fe filter were consistently below the drinking water standard (DWS) for Fe(II) of 0.3 mg/L. Dissolved Fe(II) was removed from the groundwater prior to Mn biofiltration consistently over the course of the field experiment (183 days).

Figure 1(b) presents changes in the Mn(II) concentrations in the Mn filter effluent over time. Figure 1(c) shows the effluent temperatures monitored at the outlet of the Mn filter. Mn(II) concentrations in the Mn filter effluent were relatively stable over the first month (days 0–29) at ~0.8 mg/L, which was only ~0.1 mg/L less than the Mn(II) concentration in the influent groundwater (0.88 ± 0.01 mg/L). However, between days 29 and 34, Mn(II) concentrations began to decrease in the Mn filter effluent (Figure 1(b)). Meanwhile, the effluent temperatures were stable at 8 °C for the first 81 days of the biofiltration experiment, indicating that Mn(II) removal commenced in 29–34 days at the on-site temperature of 8 °C. Two additional months were required to reach the steady-state functioning of the Mn filter at 97 days, at which point the Mn(II) removal efficiency was high and stable (97 ± 0.9%). The mean effluent temperature during the steady-state functioning period was 12 ± 0.6 °C.

Mn(II) concentrations in the Mn filter effluent collected at the site were 0.03 ± 0.01 mg/L during the steady-state functioning period. The ICP-OES analyses for the effluent collected on day 110 confirmed that total Mn(II) concentrations in the effluent were below the DWS of 0.05 mg/L (Table 1). The difference in the datasets for mean total Mn(II) concentrations in the groundwater before and after biofiltration was statistically significant, with $p < 0.0001$ (t-test, Table 1). The LBB I assay (Figure 1(e)) provided an on-site indication of Mn-oxide formation on the anthracite and sand collected from the Mn filter on day 183 (at the end of the experiment). Mn(II) oxidation in the Fe filter was negligible, as indicated by the LBB I assay for the filter media collected from the Fe filter (Figure 1(d)). Total Mn concentrations in the Fe filter effluent (day 110) were as high as 0.84 mg/L. This is most likely due to the lower redox potential in the Fe filter (e.g., <200 mV), which allows Fe(II) oxidation but not Mn(II) oxidation (Mouchet 1992). $NH_3$ concentrations were as low as 0.53 mg/L in the groundwater influent, and nitrifying activity would not prevail in the Fe filter.

After Mn(II) removal began at 8 °C and shortly before the start of steady-state functioning in the Mn biofilter, the effluent temperature increased from 8 to 13 °C due to indoor heating in the water treatment facility in October (Figure 1(c)). There was no direct heat supply to the biofiltration units. After October, effluent temperatures fluctuated between 9.5 and 14.8 °C until early December (after the steady-state condition was reached), and then stabilized at 11 ± 0.6 °C for the rest of the winter period (until January), during which the Mn(II) removal efficiency of the Mn filter was still stable at 97% and was not influenced by the temperature fluctuations (Figure 1(b) and 1(c)).

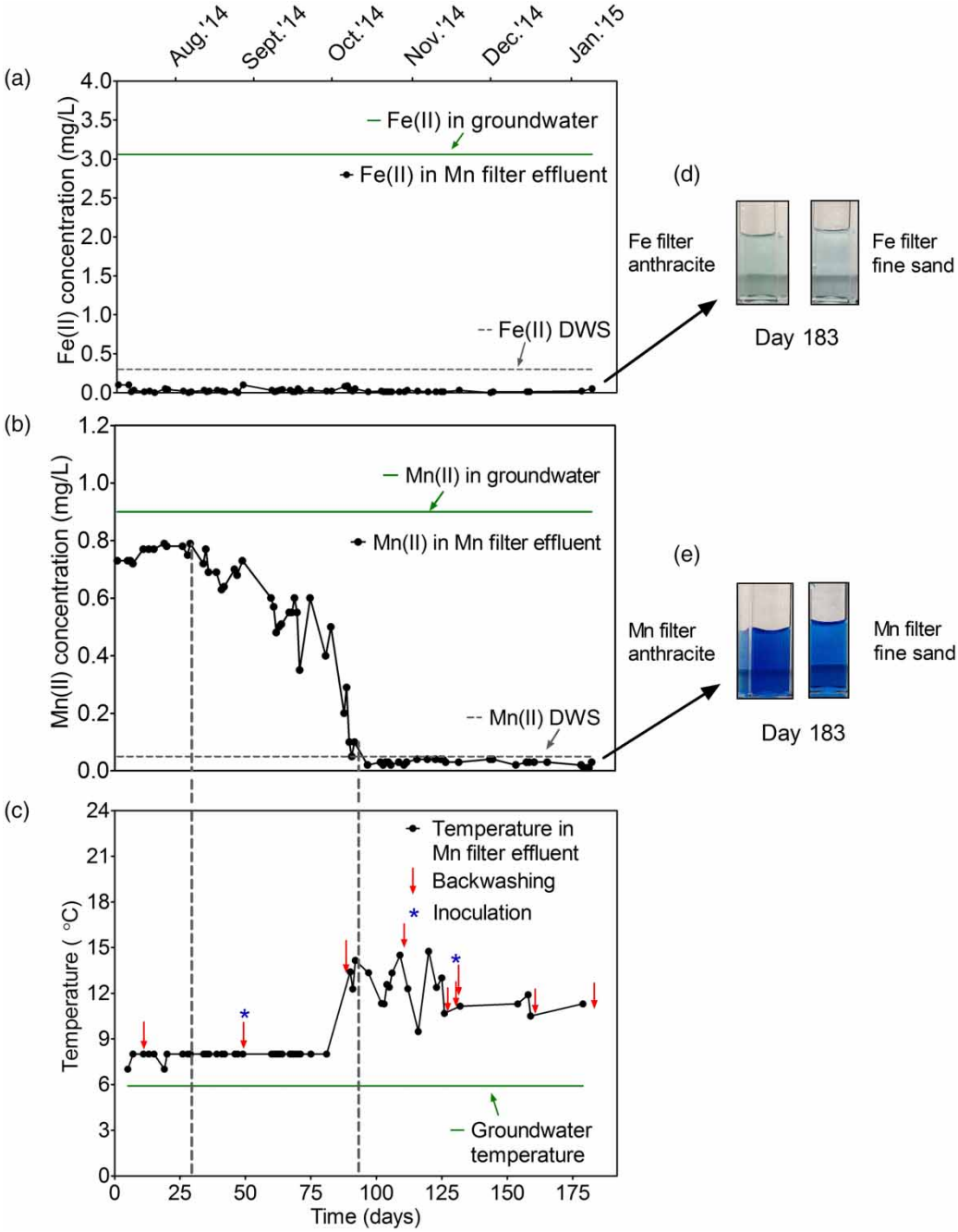


**Figure 1** | Profiles of Fe(II) and Mn(II) concentrations, and temperatures measured from the effluent stream of the Mn filter. Downward arrows represent backwashes during the course of the biofilter operation. Asterisks (*) represent inoculations of the Mn filter with backwash sludge. DWS refers to the Canadian drinking water standards of 0.3 and 0.05 mg/L for Fe(II) and Mn(II), respectively. Leucoberbelin blue I (LBB I) assay indicated Mn (III/IV) oxides desorbed from anthracite and sand collected from the Fe and Mn filters.

## Shift in ORP

The ORP in the Mn filter gradually increased as the Mn(II) concentrations decreased in the Mn filter effluent stream (Figure 2(a)). This correlation was statistically significant based on a Spearman correlation analysis (correlation coefficient: −0.84, $p < 0.0001$). Once the ORP in the Mn filter reached 300 and 313 mV around days 29 and 34, Mn(II)

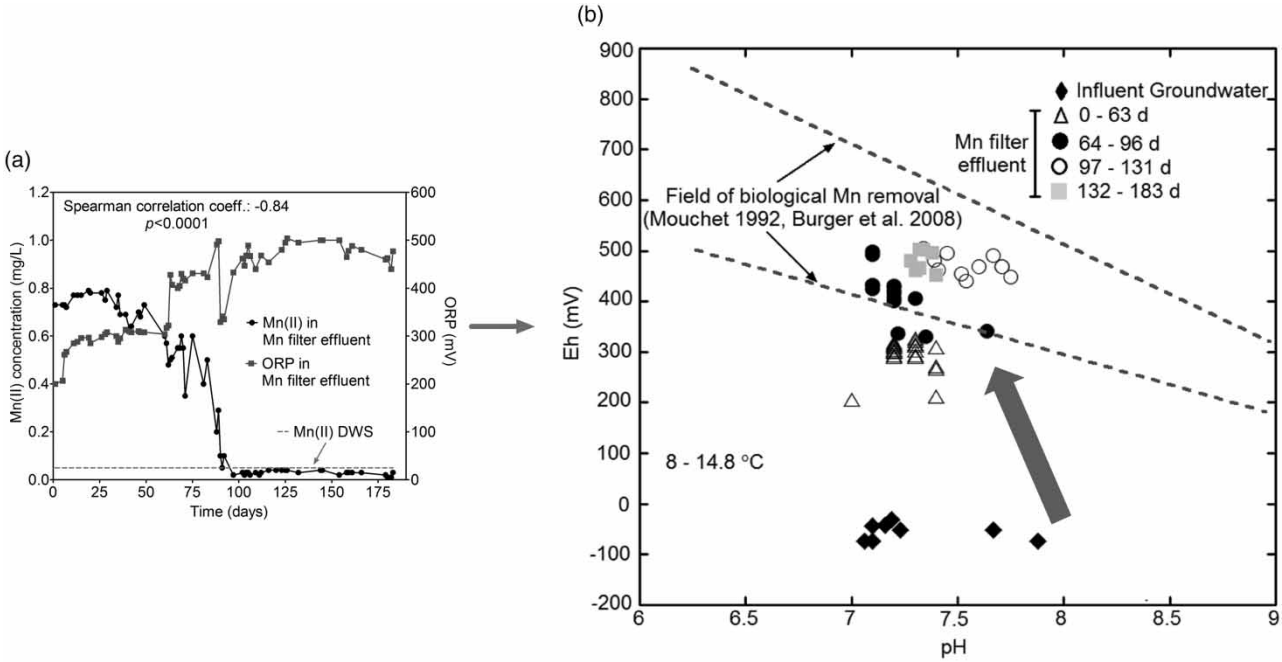


**Figure 2** | The correlation between changes in Mn(II) concentrations and ORP. The Eh-pH diagram indicates a shift in Eh and pH conditions in favor of biological Mn(II) oxidation.

removal commenced as described above (Figure 2(a)). A steep increase in the ORP from ~300 to ~430 mV was observed shortly after a filter backwash with a subsequent inoculation of the Mn biofilter with the backwashed sludge. At that point, the ORP remained over 400 mV and became relatively stable between 400 and 500 mV. Once the steady-state functioning of the Mn filter was established, the ORP was less sensitive to both temperature fluctuations and backwashing frequency (Figures 1(c) and 2(a)).

Using the ORP and corresponding pH data measured from the influent groundwater and Mn filter effluent, Pourbaix diagrams (Mn-$H_2O$ system) were constructed (Figure 2(b)). The Eh (or ORP) and pH conditions of the Mn filter notably shifted from reducing to oxidizing conditions over the course of biofiltration. As the Mn filter acclimated, Eh-pH conditions in the Mn filter gradually shifted to conditions suited for biological Mn(II) oxidation, as similarly reported by Mouchet (1992) and Pacini *et al.* (2005). Once the steady-state functioning of the Mn filter was reached (after 97 days), all Eh-pH data points fell within the field of *biological* Mn(II) removal. The shift in the redox conditions and pH in the Mn filter suggested the enhancement of biological Mn(II) oxidation.

The co-presence of Fe(II), $NH_3$, DO concentrations, and pH were not within their limiting ranges for biological Mn(II) oxidation (Table 1). The DO content in the Mn filter was maintained at 9 ± 1.7 mg/L. An increase in nitrate ($NO_3^-$) concentrations from 0.04 to 1.8 mg/L was observed during biofiltration. However, nitrification did not appear to inhibit Mn(II) oxidation in the Mn filter, presumably due to the low initial concentrations of $NH_3$.

## Viability and metabolic activity of microbial populations

The viable populations of aerobic MnOB in the effluent and backwash water of the Mn filter (collected on day 110, early in the period of steady-state functioning) were significantly greater than in the untreated groundwater (also sampled on day 110), based on the plate-count enumerations of MnOB at the start-up temperature of 8 °C (Figure 3(a); one-way ANOVA, $p < 0.0001$). Similarly, the MPN data for day 106 samples showed that a greater number of culturable heterotrophs were present in the Mn filter effluent (93 MPN/mL) than in the raw influent groundwater (2 MPN/mL) and the Fe filter effluent (59 MPN/mL). The ATP concentrations measured after the experiment in the

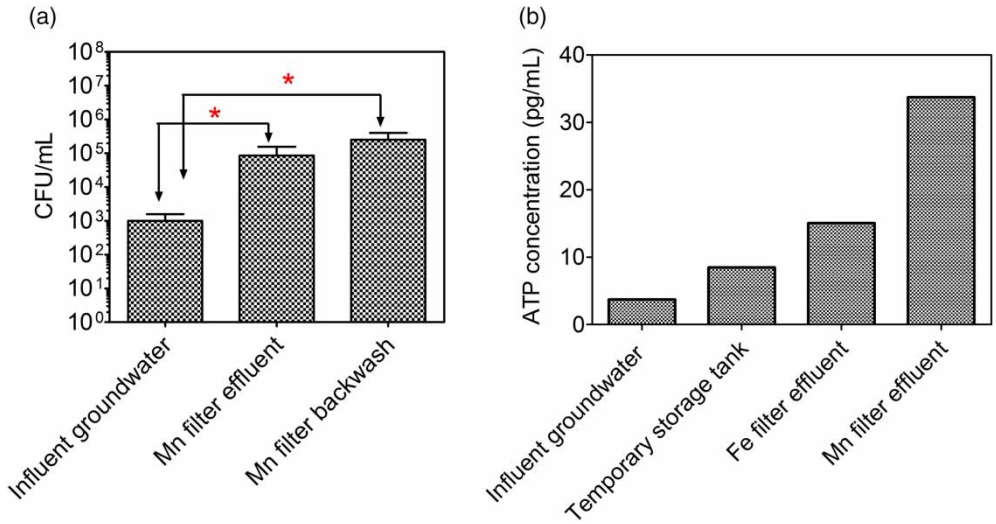


**Figure 3** | (a) Viable Mn(II)-oxidizing bacteria in the Mn-filter effluent on Day 110, enumerated at 8 °C. (b) ATP concentrations.

groundwater, storage reservoir, Fe filter effluent, and Mn filter effluent indicated that ATP was notably elevated in the Mn filter effluent, indicating that microbial metabolic activity continued throughout the period of steady-state functioning (Figure 3(b)).

## Cold-adapted MnOB consortium

The additional culturing experiment using backwash water collected on day 110 was conducted to identify a culturable MnOB consortium adapted to the start-up temperature (8 °C), and to visually observe biogenic Mn oxide formation. The backwash water used for the experiment was collected when the ORP of the Mn filter exceeded 400 mV (Figure 2(b)). The MnOB consortium from the backwash water was able to rapidly produce biogenic Mn oxides within five days at 8 °C (Figure 4). The EDS analysis detected Mn in the precipitates (Figure 4(d)). The SEM images showed poorly crystalized precipitates with amorphous morphology, which is characteristic of biogenic Mn oxides (Figure S2, available with the online version of this paper). The Mn-bearing solid precipitates exhibited a ΔH of 394 gauss, centered at a g-factor of 2.0, confirming the *biogenic* origin of the Mn oxides (Figure 4(e)). Conversely, the ΔH and g-factor of chemically synthesized birnessite mineral (standard) were 2,816 gauss and 2.0, respectively, indicating an *abiotic* origin for the Mn oxides (Figure S3, available with the online version of this paper). The rapid formation of biogenic Mn oxides at 8 °C reflected that the Mn filter had biologically acclimated at the varying low on-site temperatures. Even for filter media that were pre-coated with Mn oxides in other Mn(II)-removal studies, temperatures below 15 °C (especially below 10 °C) still significantly decreased the Mn(II) removal efficiencies (Jia *et al.* 2015; Cooley & Knocke 2016).

The *Illumina*-MiSeq 16S rRNA gene sequencing analysis for the microbial consortium identified known MnOB genera, *Pseudomonas, Leptothrix, Flavobacterium*, and *Zoogloea* (highlighted in bold font in Figure 4(c)). Approximately 60% of the microbial consortium is composed of known MnOB from the literature, based on the relative abundances of the genera as percentages of the amplicon sequence reads. Of these, *Pseudomonas, Leptothrix*, and *Flavobacterium* have been frequently reported in Mn biofiltration studies (Tekerlekopoulou *et al.* 2013; Cai *et al.* 2015). However, the microbial consortium includes other diverse populations (over 46 genera), including the genera *Rhodocista* (11.3%), *Phaselicystis* (7.3%), *Bdellovibrio* (5.1%), and *Hydrogenophaga* (<2.5%).

## Accelerated Mn(II) removal and filter media ripening

After the multiple backwashes and inoculation of the Mn filter with biologically aged backwash sludge collected at

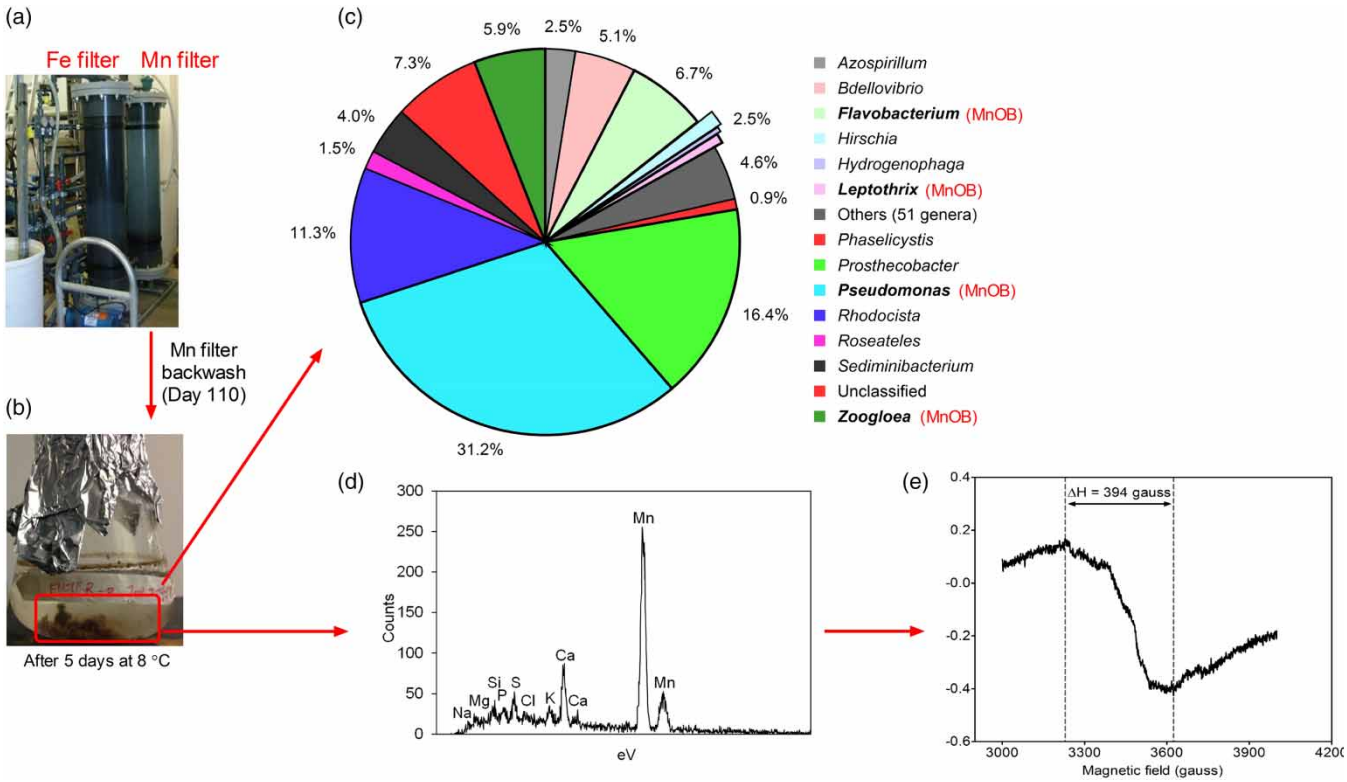


**Figure 4** | (a) The field biofiltration unit. (b) The formation of precipates in the backwash water after 5 days in a culturing flask, beginning immediately after the backwash water was collected from the Mn filter on day 110 (steady-state functioning period). (c) The relative abundance of genera as a percentage of high-throughput amplicon sequence reads from the microbial consortium enriched at 8 °C. Known MnOB genera are presented in bold. (d) The energy dispersive spectroscopy (EDS) analysis for the detection of Mn-rich precipiates. (e) The EPR analyses for solid precipiates formed in the culturing flasks of the MnOB consortium, containing biogenic Mn oxides ($\Delta H = 394$ gauss).

high ORP values of +400 mV – representing the strong activity of acclimated MnOB and rapid biogenic Mn-oxide formation – a drastic increase in the first-order rate constant ($k$) for Mn(II) removal was observed, an increase of up to five orders of magnitude (Figure 5(d)). The $k$ values were as low as $10^{-6}$ to $10^{-5}$ $min^{-1}$ between day 97 (the beginning of steady-state functioning) and day 127. The $k$ value rose steeply to 0.21 $min^{-1}$ immediately after the multiple backwashes and backwash sludge inoculation on days 127 to 132 (Figure 5(d)). The corresponding half-life ($t_{1/2}$) for Mn(II) removal was substantially reduced from ~40 days on day 92 (before the acceleration) to 3.31 min on day 159 (after the acceleration).

In particular, the acceleration of Mn(II) removal kinetics in the Mn filter was observed in the middle of steady-state functioning, at a time when high Mn(II) removal efficiencies had already been observed (Figure 5(d)). This finding indicates that tracking Mn(II) removal efficiency does not adequately take into account the ripening of the filter media. Figure 6 shows that $k$ values were as low as 0.007 to 0.068 $min^{-1}$ between days 132 and 148, even though the Mn filter exhibited the 97% removal efficiency due to the ripened bottom layers. Low $k$ values reflected the incomplete ripening of the filter media. The drastically accelerating Mn(II) removal kinetics correlated to the progressive vertical ripening of the Mn filter media. The filter ripening progressed from the bottom (gravel), to the middle (sand), and to the top (anthracite), likely due to accumulating precipitates, biomass and/or sludge solids at the bottom (Figure 6). The different types of filter media did not significantly affect biofilter ripening. As the $k$ value for Mn(II) removal reached 0.21 $min^{-1}$ with a short half-life of 3.31 min, Mn(II) from the influent groundwater was depleted rapidly as it passed through the topmost layers of the Mn filter (as specifically shown at 159 days in Figure 6). At this stage, the Mn filter was

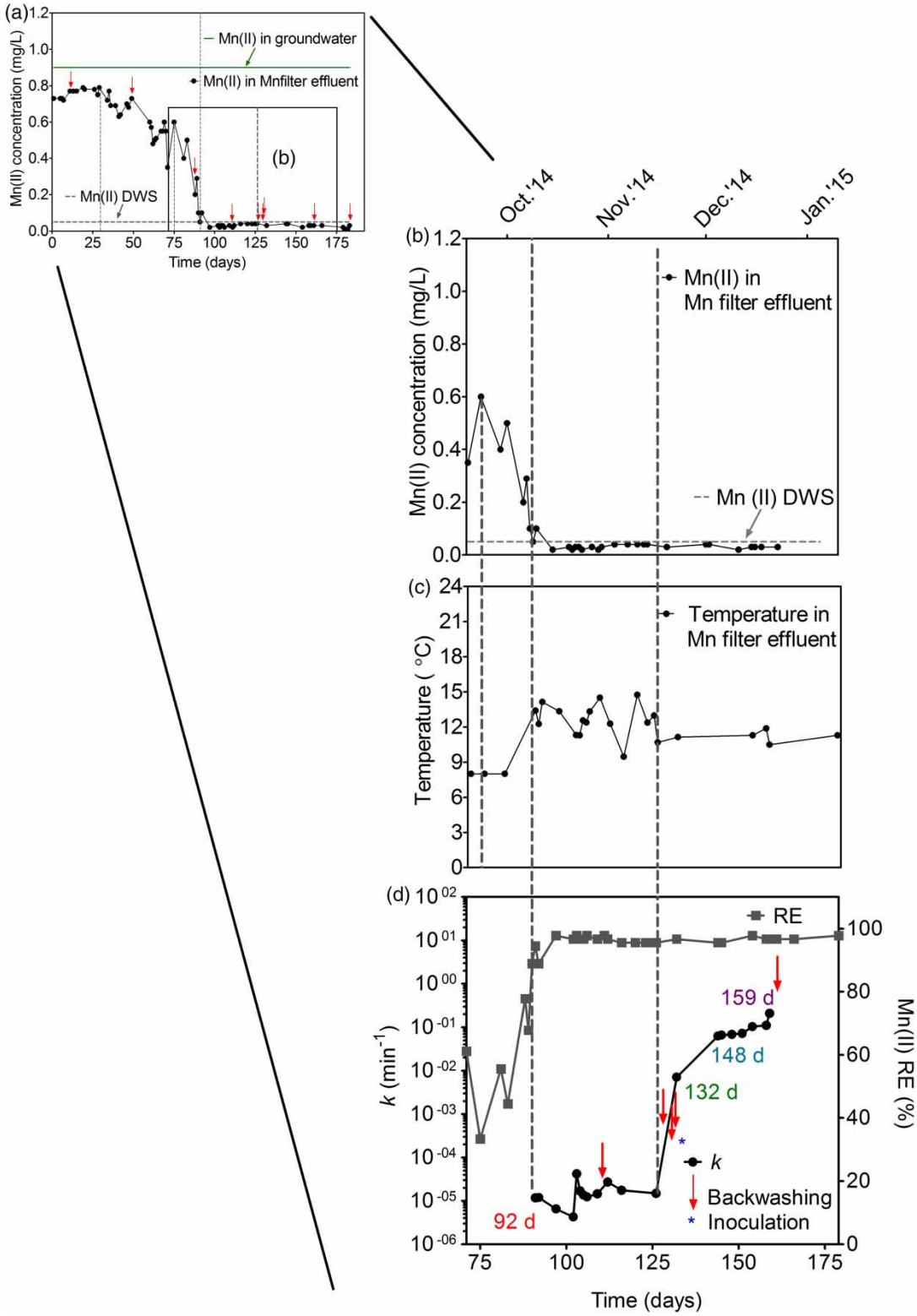


**Figure 5** | (a) Mn(II) concentration profile, (b) Mn(II) concentration profile focused on the period of steady-state functioning, (c) the corresponding temperature profile for the Mn filter effluent, and (d) changes in the Mn(II) removal efficiency (RE) and the first-order rate constant (*k*) for Mn(II) removal.

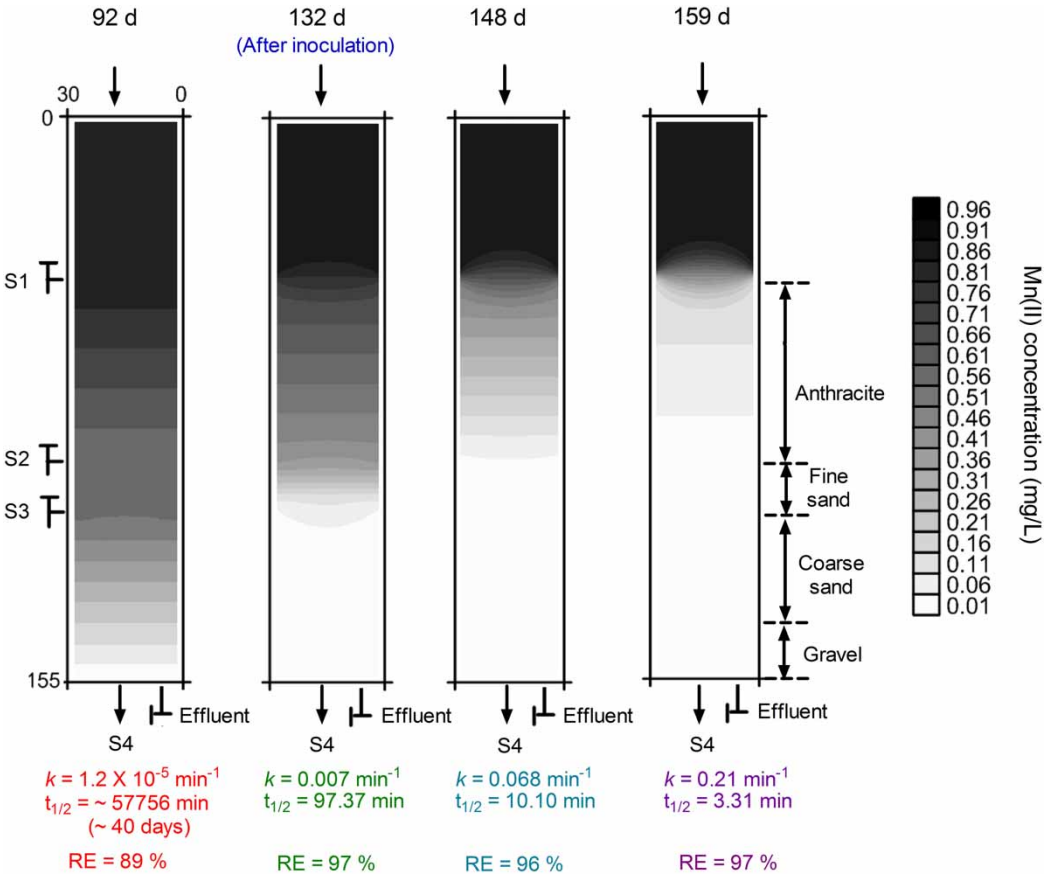


**Figure 6** | Temporal changes in the vertical profiles of Mn(II) concentrations along the depth of the Mn filter over time, indicating the ripening of the filter media.

considered nearly fully ripened based on the maturation of Mn(II) removal kinetics.

The findings presented herein are important from a field perspective. Tracking changes in the EBCT-based rate constant for Mn(II) removal is a simple approach to indicating filter ripening that is sufficiently advanced to trigger meaningful Mn(II) removal under low temperature regimes, and to determining the effective ripening period required for a biofilter. During the period of accelerated Mn(II) removal, the Mn filter effluent temperatures were very stable at $11 \pm 0.6\,^{\circ}C$ (Figure 5(c) and 5(d)). The on-site low temperature of $11\,^{\circ}C$ did not limit the acceleration of Mn(II) removal. The first-order rate constant of $0.21\ min^{-1}$ obtained after filter ripening in this study is comparable to rate constants for Mn(II) removal reported in previous Mn-biofiltration studies conducted at a wide range of temperatures. Some of those studies were conducted at warmer temperatures and with pre-aged Mn filter materials (Table 2). The four-month aging period in this study was shorter than those in previous studies (Table 2).

## Birnessite and pyrolusite formation, and surface morphology

Birnessite (K-rich $MnO_2$; Mn(IV) oxide) and pyrolusite ($\beta$-$MnO_2$; Mn(IV) oxide) were detected in the anthracite collected on day 183 (end of the experiment), confirming that the Mn filter was fully ripened with Mn oxides with the highest Mn oxidation states based on the Mn oxidation pathway (Figure 7(c)). The Mn oxidation states exhibited by birnessite and pyrolusite were +3.5 to +3.9, and +4, respectively.

**Table 2** | Comparison of rate constants ($k$) from this study and various other Mn biofilter designs

| Temperature (°C) | $k$ ($min^{-1}$) | Flow velocity ($m\ h^{-1}$) | Experiment type | Scale | Initial filter media status | Aging characteristics | Reference |
|---|---|---|---|---|---|---|---|
| – | 0.17 | 7 | Field | Full-scale | Aged | 8-month pre-aging | Katsoyiannis & Zouboulis (2004) |
| 11.2–14.6 | 0.50[a] | 10–22 | Field | Pilot-scale | Aged | 8-month pre-aging | Štembal *et al.* (2005) |
| 18–22[b] | 0.14–0.16[c] | – | Lab | Lab scale | Virgin | MnOB pre-inoculation | Cai *et al.* (2015) |
| – | 0.53[c] | 7–19 | Lab | Pilot-scale | Virgin | Aged using synthetic Mn(II)- and As(III)-contaminated water | Yang *et al.* (2015) |
| 30[b] | 0.023[c] | 0.033–0.039 | Field | Pilot-scale | Virgin | 5-month aging | Zeng *et al.* (2015) |
| 8[b] | 0.69[c] | – | Field | Pilot-scale | Manganese sand | 18-month pre-aging | Cheng *et al.* (2016) |
| 4–8[b], 8–14.8[d] | 0.21[c] | 3.21 | Field | Pilot-scale | Virgin | 4-month aging: ORP: $>+400$ mV, Abundant MnOB, Mn oxide formation | This study |

[a]Treatability factor using mass-transfer-limited kinetics.
[b]Influent water temperature.
[c]First-order rate constant.
[d]Effluent temperature.

Hausmannite ($Mn_3O_4$; Mn(III) oxide) with Mn oxidation state +2.7 (Bruins *et al.* 2015b) was detected in centrifuged backwash water collected on day 110 (early steady-state functioning period).

The ripened anthracite collected from the Mn filter on day 183 was coated mainly by Mn-rich substances with a repetitive coral-like morphology (Figure 7(b)). This surface morphology is similar to that of birnessite formed by autocatalytic Mn(II) oxidation based on visual comparisons of SEM images (Jiang *et al.* 2010; Bruins *et al.* 2015a). However, variations in the surface morphologies of Mn-rich coatings on the ripened filter media were easily observable on day 183 (Figure 7(a) and 7(b)). The SEM images of some surfaces of the ripened anthracite indicated a birnessite-like surface morphology that contains fewer coral-like patterns and appears to be fluffier (Figure 7(a)). Such a morphology has been similarly observed for biogenic Mn-oxide coatings also reported by Bruins *et al.* (2015a) and Jiang *et al.* (2010). There was no detection of Mn oxides in the virgin anthracite samples (control) (Figure 7(c) and Figure S4, available with the online version of this paper). Considering the multiple lines of evidence of enhanced biological Mn(II) oxidation, varying birnessite-like surface-coating morphologies reflected microbially mediated autocatalytic signatures of Mn(II) oxidation. Birnessite acts as an autocatalyst for physico-chemical Mn(II) oxidation (Bruins *et al.* 2015b). The detection of birnessite (crystalized) in the ripened filter media, which were largely coated by birnessite-like substances, may be connected to the accelerated Mn(II) removal kinetics observed in this biofiltration study.

## CONCLUSIONS

In the Mn filter, biological Mn(II) oxidation was significantly enhanced, which was observed using multiple indicators. In the early stage of Mn(II) biofiltration, however, the Mn filter exhibited lower $k$ values ranging from $10^{-6}$ to $10^{-5}\ min^{-1}$ at the variable on-site temperatures (8–14.8 °C). Immediately after multiple backwashes and the inoculation of the biofilter with biologically acclimated backwash sludge, $k$ values markedly increased to $0.21\ min^{-1}$ at $11 \pm 0.6$ °C, which is comparable to $k$ values obtained at higher temperatures in previous studies. The drastically accelerating $k$ for Mn(II) removal was correlated to the vertical progression of filter media ripening.

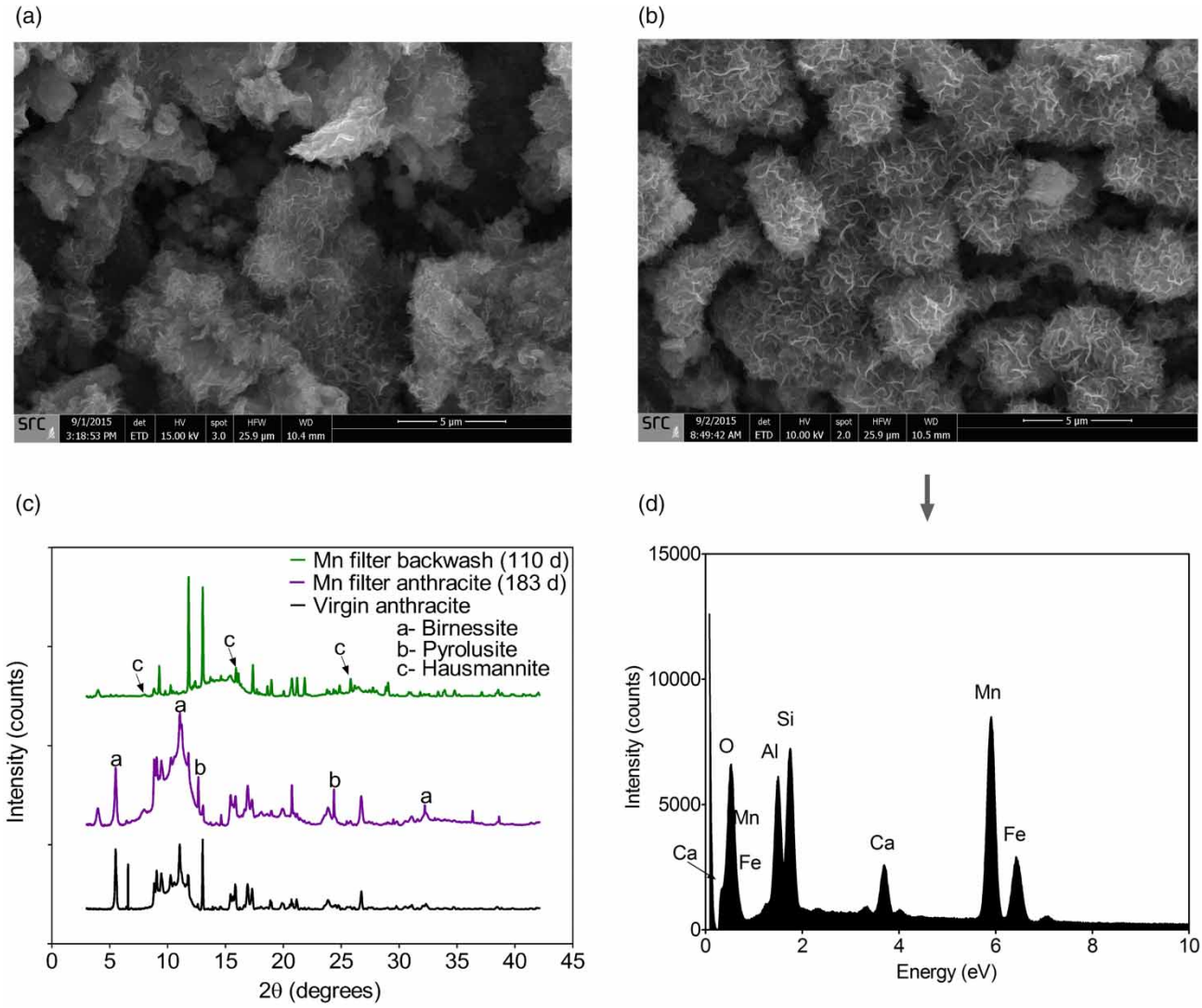


**Figure 7** | SEM images of (a) slightly ripened and (b) well ripened surfaces within the same anthracite sample collected on day 183, (c) synchrotron-based PXRD data, and (d) EDS analyses for detecting elemental metals on the ripened anthracite.

The PXRD analyses detected birnessite and pyrolusite with high Mn oxidation states ranging from +3.5 to +4 in the ripened filter media. The varying surface morphologies of the ripened filter materials exhibited combined biological *and* autocatalytic signatures. The MnOB microbial consortium capable of rapidly producing biogenic Mn oxides at the start-up temperature of 8 °C was obtained from the biologically aged backwash water. These findings have important implications for improving biofiltration in cold regions, and represent a potential breakthrough for accelerating Mn(II) oxidation kinetics in cold groundwater.

## ACKNOWLEDGEMENTS

We acknowledge technical and financial support provided by the Delco Water Division of Delco Automation Inc. This research was also funded by the Natural Sciences and Engineering Research Council of Canada (NSERC; EGP

468673-14 and RGPIN-2014-05902), Mitacs (Mitacs-Accelerate Graduate Research Internship, IT06847), and the Canada Foundation for Innovation (CFI; JELF#33982). The synchrotron-based PXRD analyses described in this study were performed at the Canadian Light Source (CLS), which is supported by the NSERC, the National Research Council Canada, the Canadian Institutes of Health Research, the Province of Saskatchewan, Western Economic Diversification Canada, and the University of Saskatchewan. We thank Dr Michel Fodje, Dr Viorica Bondici, and Samira Sumaila for technical support during the PXRD analyses, and the CLS for granting access to their analytical equipment in the Life Sciences Laboratory. We also thank Dr Ramaswami Sammynaiken for the EPR analyses at the Saskatchewan Structural Sciences Centre at the University of Saskatchewan.

## REFERENCES

Berbenni, P., Pollice, A., Canziani, R., Stabile, L. & Nobili, F. 2000 Removal of iron and manganese from hydrocarbon-contaminated groundwaters. *Bioresource Technology* **74** (2), 109–114.

Boogerd, F. C. & de Vrind, J. P. 1987 Manganese oxidation by *Leptothrix discophora*. *Journal of Bacteriology* **169** (2), 489–494.

Bruins, J. H., Petrusevski, B., Slokar, Y. M., Huysman, K., Joris, K., Kruithof, J. C. & Kennedy, M. D. 2015a Biological and physico-chemical formation of Birnessite during the ripening of manganese removal filters. *Water Research* **69**, 154–161.

Bruins, J. H., Petrusevski, B., Slokar, Y. M., Kruithof, J. C. & Kennedy, M. D. 2015b Manganese removal from groundwater: characterization of filter media coating. *Desalination and Water Treatment* **55** (7), 1851–1863.

Burger, M. S., Mercer, S. S., Shupe, G. D. & Gagnon, G. A. 2008 Manganese removal during bench-scale biofiltration. *Water Research* **42** (19), 4733–4742.

Cai, Y. a., Li, D., Liang, Y., Luo, Y., Zeng, H. & Zhang, J. 2015 Effective start-up biofiltration method for Fe, Mn, and ammonia removal and bacterial community analysis. *Bioresource Technology* **176**, 149–155.

Cai, Y. a., Li, D., Liang, Y., Zeng, H. & Zhang, J. 2016 Operational parameters required for the start-up process of a biofilter to remove Fe, Mn, and $NH_3$-N from low-temperature groundwater. *Desalination and Water Treatment* **57** (8), 3588–3596.

Cheng, Q., Nengzi, L., Xu, D., Guo, J. & Yu, J. 2017 Influence of nitrite on the removal of Mn(II) using pilot-scale biofilters. *Journal of Water Reuse and Desalination* **7** (3), 264–271.

Cooley, R. & Knocke, W. R. 2016 Low-temperature effects on the removal of soluble manganese in MnOx(s)-coated media systems. *Journal of Water Supply: Research and Technology – AQUA* **65** (8), 626–634.

Fortin, G., van der Kamp, G. & Cherry, J. A. 1991 Hydrogeology and hydrochemistry of an aquifer-aquitard system within glacial deposits, Saskatchewan, Canada. *Journal of Hydrology* **126** (3), 265–292.

Granger, H. C., Stoddart, A. K. & Gagnon, G. A. 2014 Direct biofiltration for manganese removal from surface water. *Journal of Environmental Engineering-ASCE* **140** (4), 04014006 (1–8).

Jia, H., Liu, J., Zhong, S., Zhang, F., Xu, Z., Gong, X. & Lu, C. 2015 Manganese oxide coated river sand for Mn(II) removal from groundwater. *Journal of Chemical Technology and Biotechnology* **90** (9), 1727–1734.

Jiang, S., Kim, D. G., Kim, J. & Ko, S. O. 2010 Characterization of the biogenic manganese oxides produced by *Pseudomonas putida* strain MnB1. *Environmental Engineering Research* **15** (4), 183–190.

Katsoyiannis, I. A. & Zouboulis, A. I. 2004 Biological treatment of Mn(II) and Fe(II) containing groundwater: kinetic considerations and product characterization. *Water Research* **38** (7), 1922–1932.

Krishnan, K. P., Sinha, R. K., Krishna, K., Nair, S. & Singh, S. M. 2009 Microbially mediated redox transformations of manganese(II) along with some other trace elements: a study from Antarctic lakes. *Polar Biology* **32** (12), 1765–1778.

Mouchet, P. 1992 From conventional to biological removal of iron and manganese in France. *Journal of the American Water Works Association* **84** (4), 158–167.

Pacini, V. A., María Ingallinella, A. & Sanguinetti, G. 2005 Removal of iron and manganese using biological roughing up flow filtration technology. *Water Research* **39** (18), 4463–4475.

Schloss, P. D., Westcott, S. L., Ryabin, T., Hall, J. R., Hartmann, M., Hollister, E. B., Lesniewski, R. A., Oakley, B. B., Parks, D. H., Robinson, C. J., Sahl, J. W., Stres, B., Thallinger, G. G., Van Horn, D. J. & Weber, C. F. 2009 Introducing mothur: opensource, platform-independent, community-supported software for describing and comparing microbial communities. *Applied and Environmental Microbiology* **75** (23), 7537–7541.

Štembal, T., Markić, M., Ribičić, N., Briški, F. & Sipos, L. 2005 Removal of ammonia, iron and manganese from groundwaters of northern Croatia – pilot plant studies. *Process Biochemistry* **40** (1), 327–335.

Tebo, B. M., Johnson, H. A., McCarthy, J. K. & Templeton, A. S. 2005 Geomicrobiology of manganese(II) oxidation. *Trends in Microbiology* **13** (9), 421–428.

Tebo, B. M., Clement, B. G. & Dick, G. J. 2007 Biotransformations of manganese. In: *Manual of Environmental Microbiology*, 2nd edn (C. J. Hurst, R. L. Crawford, J. L. Garland, D. A.

Lipson, A. L. Mills & L. D. Stetzenbach, eds). ASM Press, Washington, DC, pp. 1223–1238.

Tekerlekopoulou, A. G., Pavlou, S. & Vayenas, D. V. 2013 Removal of ammonium, iron and manganese from potable water in biofiltration units: a review. *Journal of Chemical Technology and Biotechnology* **88** (5), 751–773.

Yang, H., Sun, W., Ge, H. & Yao, R. 2015 The oxidation of As(III) in groundwater using biological manganese removal filtration columns. *Environmental Technology* **36** (21), 2732–2739.

Zeng, X., Xia, J., Wang, Z. & Li, W. 2015 Removal of iron and manganese in steel industry drainage by biological activated carbon. *Desalination and Water Treatment* **56** (9), 2543–2550.

First received 6 February 2017; accepted in revised form 20 July 2017. Available online 10 October 2017